Journal of the European Ceramic Society xxx (xxxx) xxx

Contents lists available at ScienceDirect

Journal of the European Ceramic Society

journal homepage: www.elsevier.com/locate/jeurceramsoc

Original Article

Improved tri-layer microwave dielectric ceramic for 5 G applications

Shun Wang [a,b,1], Weijia Luo [a,b,1], Lingxia Li [a,b,*], Mingkun Du [a,b], Jianli Qiao [a,b]

[a] School of Microelectronics, Tianjin University, Tianjin 300072, China
[b] Key Laboratory for Advanced Ceramics and Machining Technology of Ministry of Education, Tianjin University, Tianjin 300072, China

ARTICLE INFO

Keywords:
Tri-layer ceramic
Microwave dielectric properties
Cooperative optimization

ABSTRACT

Tri-layer $ZnTi_{0.97}Ge_{0.03}Nb_2O_8$-$TiO_2$-$ZnTi_{0.97}Ge_{0.03}Nb_2O_8$ ceramics with different mass fractions of TiO_2 were initially prepared. The advantages of the multilayer architecture were fully demonstrated, and the microwave dielectric properties were controlled by the components of each dielectric layer. In contrast to the random distribution-type $ZnTi_{0.97}Ge_{0.03}Nb_2O_8$-$TiO_2$, this tri-layer architecture could achieve a nearly 50 % increase in the $Q\times f$ value. Meanwhile, based on the parallel distribution mode, a 10 % increase in the dielectric constant could be obtained due to the existence of Zn_2GeO_4. After sintering at 1120 ℃ for 6 h, $ZnTi_{0.97}Ge_{0.03}Nb_2O_8$-$TiO_2$-$ZnTi_{0.97}Ge_{0.03}Nb_2O_8$ tri-layered ceramics exhibited excellent dielectric properties ($\varepsilon_r = 42.1$, $Q\times f = 51{,}477$ GHz and $\tau_f = +1.9$ ppm/℃) with 0.04 wt% TiO_2, and the cooperative optimization of microwave dielectric properties was achieved. This research provides a direction for the preparation of high-performance microwave dielectric resonators for application in 5 G wireless communication technologies.

1. Introduction

To better meet the requirements of high-performance dielectric devices in the 5 G era for low insertion loss, small size, and good temperature stability, the quality factor value ($Q\times f$ value), dielectric constant (ε_r), and the temperature coefficient of resonant frequency (τ_f) of the corresponding microwave dielectric ceramics (MWDCs) should be further optimized. However, the relation between the $Q\times f$ value, ε_r, and τ_f of MWDCs is mutually restricted, and improving the comprehensive dielectric performance of MWDCs has been the focus of past research [1–4]. At present, the two-phase composite method is widely used to prepare high-performance MWDCs [1,5,6]. That is, the microwave dielectric performance can be adjusted by adding another phase with high ε_r and opposite τ_f [5,6]. This random distribution mode is a typical combination mode for MWDCs with different phases, which means that the required materials are directly mixed and turned into ceramics. Based on this method, both the dielectric constant and the temperature coefficient of resonance frequency can be optimized. Nevertheless, undesired chemical reactions between the two mixed materials inevitably lead to varied defects that deteriorate the microwave dielectric properties, and the products cannot meet the application requirement of low insertion loss [7–12].

Recently, the laminated co-firing method has been used to prepare microwave dielectric ceramics with two complementary phases [13–15]. For instance, $Zn_{1.01}Nb_2O_6/TiO_2/Zn_{1.01}Nb_2O_6$ and $MgTiO_3/TiO_2/MgTiO_3$ laminated co-fired ceramics with excellent characteristics were reported by Zhang et al. [16,17]. This method can effectively reduce the deterioration of the $Q\times f$ value during the adjustment process of ε_r and τ_f. However, the ε_r of the system increases slightly, which is not conducive to the miniaturization of the microwave device. Therefore, eliminating the defects of the two methods has become an important topic.

$ZnTiNb_2O_8$ was discovered in the $ZnNb_2O_6$-TiO_2 system by Baumgarte et al. [18]. Kim et al. [19] first reported the microwave dielectric properties of sintering at 1250 ℃: $Q\times f = 42{,}500$ GHz, $\varepsilon_r = 43$, and $\tau_f =$ -50 ppm/℃. The insufficient $Q\times f$ value and the large negative temperature coefficient of resonance frequency limit its application in 5 G communication. Recently, Luo et al. [20] optimized its quality factor ($Q\times f$ value) nearly 1.5 times through Ge^{4+} quantitative doping ($Q\times f =$ 62700, $\varepsilon_r =$35.6, and $\tau_f =$ -58 ppm/℃ with 3 mol% Ge^{4+} doped in $ZnTiNb_2O_8$). However, its temperature coefficient still needs to be improved. Therefore, based on their phase compositions, the above-mentioned methods were chosen to tailor the comprehensive dielectric performance of $ZnTi_{0.97}Ge_{0.03}Nb_2O_8$ with multiple phases.

In this paper, $ZnTi_{0.97}Ge_{0.03}Nb_2O_8$ based on our previous work is used as the matrix, and the composite ceramic ($ZnTi_{0.97}Ge_{0.03}Nb_2O_8$-

* Corresponding author at: School of Microelectronics, Tianjin University, Tianjin 300072, China.
E-mail address: tjulilingxia66@163.com (L. Li).
[1] Shun Wang and Weijia Luo contributed equally to this work and should be considered as co-first authors.

https://doi.org/10.1016/j.jeurceramsoc.2020.09.008
Received 15 June 2020; Received in revised form 5 September 2020; Accepted 5 September 2020

TiO_2) with a tri-layered architecture and random distribution is prepared by the above two methods. Based on analysis using XRD and SEM, the crystal structure, the phase compositions, and the microstructure of the transition layers are characterized. Then, the microwave dielectric properties of the $ZnTi_{0.97}Ge_{0.03}Nb_2O_8$-$TiO_2$-$ZnTi_{0.97}Ge_{0.03}Nb_2O_8$ tri-layer architecture ceramics are comprehensively analysed, and the modification mechanism of the co-fired layer composite method is clarified in the $ZnTiNb_2O_8$ ceramic-derived system. Meanwhile, a novel microwave dielectric ceramic with a high $Q\times f$ value, high dielectric constant, and good temperature stability is obtained. This material is expected to meet the application requirements of a high-performance dielectric resonator in the 5 G era.

2. Experimental procedure

The $ZnTi_{0.97}Ge_{0.03}Nb_2O_8$-$TiO_2$-$ZnTi_{0.97}Ge_{0.03}Nb_2O_8$ (ZTGN-TO-ZTGN) ceramic with tri-layer architecture and the $ZnTi_{0.97}Ge_{0.03}Nb_2O_8$-$TiO_2$ (ZTGN-TO) ceramic with random distribution were prepared via a solid phase calcination process. High-purity ZnO (≥99.99 %), GeO_2 (≥99.99 %), Nb_2O_5 (≥99.99 %), and TiO_2 (≥99 %) powders were selected as the raw materials. First, $ZnTi_{0.97}Ge_{0.03}Nb_2O_8$ (ZTGN) powders were pre-synthesized by the traditional solid-state method. According to the nominal composition, ZnO, TiO_2, GeO_2, and Nb_2O_5 powders were weighed and ball-milled in pure water for 6 h with zirconia balls. Then, the slurry was dried and calcined at 950 °C for 4 h in air. After the calcination process, the ZTGN powders and TiO_2 powders were re-milled with 1 wt% PVA for 12 h. Based on the compositions of 0.5ZTGN-xTO-0.5ZTGN (x = 0.01, 0.02, 0.03, 0.04, 0.05, where x is a mass ratio), the two powders were added into the mould layer by layer (in the order of ZTGN-TO-ZTGN) and then pressed into tri-layer pellets 10 mm in diameter and approximately 4∼5 mm in thickness. The green bodies of the layer co-fired ceramics are shown in Fig. 1. TiO_2 was evenly spread in the middle layer, and the samples were labelled ZTGN-xTO-ZTGN according to the amount of TiO_2 added. In addition, samples of randomly distributed ZTGN-TO dielectric ceramics were prepared by a conventional mixing process. According to the mass ratio, the pre-sintered powders were mixed with high-purity TiO_2. After that, the mixed powders were ball-milled with 1 wt% PVA for 12 h. The mixtures were dried and pressed into green pellets with a diameter of 10 mm and a thickness of 5 mm, and the samples were marked as ZTGN-yTO according to the y values (y = 0.10, 0.12, 0.14, 0.16, 0.18). Finally, the two types of samples were sintered at 1120 °C in air at a rate of 3 °C/min for 6 h.

The phase compositions of the two as-prepared samples were identified by an X-ray diffractometer (XRD, Rigaku, D/MAX-2500, Tokyo, Japan) with Cu Kα radiation. The 2theta (2θ) range was from 20° to 80°. The fracture surface microtopography and chemical composition of the lamination samples were detected by scanning electron microscopy (FESEM, FEI Nanosem 430, Oregon, North America) with an energy dispersive spectrometer (EDS). To ensure that the micrographs were representative and clear, the fracture samples were first polished with a polishing machine. The polished samples were washed using ultrasonic waves and then thermally etched for 0.5 h. Prior to imaging, the samples were sputtered with gold to ensure electroconductivity. The dielectric properties (ε_r, $Q\times f$ value, and τ_f) were examined by a network analyser

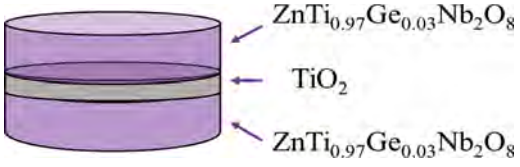

Fig. 1. Configuration diagram of the tri-layer ZTGN-TO-ZTGN green body (For interpretation of the references to colour in this figure legend, the reader is referred to the web version of this article).

(Agilent Technologies E5071C, Agilent Technologies, Singapore) accompanied by a temperature chamber. ε_r and τ_f were measured by the Hakki-Coleman dielectric resonator method, and the unloaded quality factor was measured using the cavity method. The τ_f values were calculated via the following equation:

$$\tau_f = \frac{f_2 - f_1}{f_1(85-25)} \quad (1)$$

where f_1 and f_2 are the resonant frequencies of the samples at 25 ℃ and 85 ℃, respectively. The measurement error of the dielectric constant, $Q\times f$ value, and the temperature coefficient of the resonance frequency were <0.5 %×ε_r, 2% $Q\times f$, and 0.5 × 10^{-6}/℃, respectively.

3. Results and discussion

The microwave dielectric properties of the tri-layer samples and randomly distributed samples sintered at 1120 ℃ for 6 h with different mass fractions of TiO_2 are listed in Table 1. The microwave dielectric properties of $ZnTi_{0.97}Ge_{0.03}Nb_2O_8$ and TiO_2 sintered at 1120 ℃ for 6 h are also listed. The optimized microwave dielectric properties of the two samples are ε_r = 42.1, $Q\times f$ = 51,477 GHz, and τ_f = +1.9 ppm/℃ for ZTGN-0.04TO-ZTGN and ε_r = 46, $Q\times f$ =35,049 GHz, and τ_f = -3.2 ppm/ for ZTGN-0.16TO. Under the premise of good temperature stability, the tri-layer architecture can achieve a nearly 50 % increase in the $Q\times f$ value, and the dielectric constant does not deteriorate significantly compared with the random distribution type. Unlike the layered process, the random distribution process requires a large amount of TiO_2 (four times as much as the layered process) to make the temperature coefficient of resonance frequency close to zero in this system (as shown in Table 1). This can be attributed to the formation of other phases, which is confirmed in the following analysis [21].

Fig. 2 shows the XRD patterns of the ZTGN-0.04TO-ZTGN sample (Fig. 2a), along with the sample ZTGN-0.16TO for comparison. When the sintering temperature is 1120 ℃, the main phase of both as-prepared samples is a $ZnTiNb_2O_8$ phase with an ixiolite structure (JCPDS#48−0323), and a trace Zn_2GeO_4 (JCPDS#11−0687) phase presented by the (410) diffraction peak is observed in both samples simultaneously. Only in Fig. 2a can the diffraction peak representing the TiO_2 phase with a rutile structure (JCPDS#21−1276) in the (110) direction be observed, which is difficult to find in Fig. 2b. In addition, the diffraction peak of the Ti-rich phase $Zn_{0.17}Nb_{0.33}Ti_{0.5}O_2$ (JCPDS#11−0687), which can be considered a $ZnTiNb_2O_8$-$2TiO_2$ solid solution. GeO_2 (JCPDS#23−0999) is also detected in Fig. 2b. However, no other diffraction peaks are detected except for the ixiolite phase and rutile phase in Fig. 2a. This phenomenon can be attributed to the similar structure of ixiolite and rutile phases, which results in similar reaction

Table 1
The microwave dielectric properties of samples prepared by the layered process and random distribution process.

samples	ε_r	$Q\times f$ (GHz)	τ_f (ppm/℃)
ZTGN-0.01TO-ZTGN	36.9	58,921	−46.41
ZTGN-0.02TO-ZTGN	37.8	56,314	−27.94
ZTGN-0.03TO-ZTGN	39.7	53,948	−17.62
ZTGN-0.04TO-ZTGN	42.1	51,477	+1.9
ZTGN-0.05TO-ZTGN	42.9	48,001	+12.41
ZTGN-0.10TO	38.57	51,576	−42.65
ZTGN-0.12TO	39.2	50,800	−36.5
ZTGN-0.14TO	40.2	46,000	−31.52
ZTGN-0.16TO	46	35,000	−3.2
ZTGN-0.18TO	48.9	26,572	+32.7
$ZnTi_{0.97}Ge_{0.03}Nb_2O_8$	35.6	62,700	−58
TiO_2	94.8	12,470	+427

The measurement error of dielectric constant, $Q\times f$ value and the temperature coefficient of resonance frequency was <0.5 %×ε_r, 2% $Q\times f$ and 0.5 × 10^{-6}/℃, respectively.

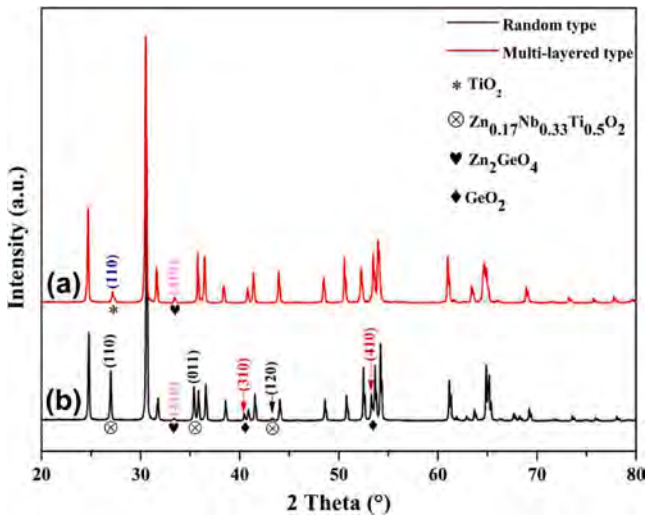

Fig. 2. XRD patterns of (a) the random type and (b) multi-layered type samples.

temperatures for the various phases. Therefore, some unexpected chemical reactions will occur between $ZnTi_{0.97}Ge_{0.03}Nb_2O_8$ and TiO_2, which give rise to unexpected secondary phases (for example, $Zn_{0.17}Nb_{0.33}Ti_{0.5}O_2$ and GeO_2), and the microwave dielectric properties are worsened [8,11,12]. On this basis, the tri-layer co-fired approach can effectively restrict the chemical reactions between $ZnTi_{0.97}Ge_{0.03}Nb_2O_8$ and TiO_2 at a finite area (shown in Fig. 4), and the microwave dielectric properties are improved significantly [13–17]. In addition, compared to the TiO_2 phase ($\tau_f = +427$ ppm/℃) with a rutile structure, $Zn_{0.17}Nb_{0.33}Ti_{0.5}O_2$ has a lower temperature coefficient of resonance frequency ($\tau_f = +237$ ppm/℃). Therefore, the random distribution process requires more titanium oxide when the τ_f values are near zero (shown in Table 1) [22,23].

To explore the mechanism by which the tri-layer co-fired ZTGN-TO-ZTGN samples influence their microwave dielectric properties, XRD data are refined and fitted to obtain the volume fraction of the rutile phase TiO_2 in the rephase system. The Rietveld refinement of the XRD data for ZTGN-0.04TO-ZTGN is shown in Fig. 3a, and the Rietveld discrepancy factors R_{wp} and Rp are all below 15 % ($R_{wp} = 12.23$ %, $R_p = 10.41$ %, GOF = 1.27). Fig. 3b illustrates the test values and theoretical values of the TiO_2 volume fraction. At a lower TiO_2 additive amount (<0.03 g), the difference between the theoretical values and the measured values of TiO_2 phase content is large, which may be caused by the formation of a transition phase through ion diffusion between the middle layers of the

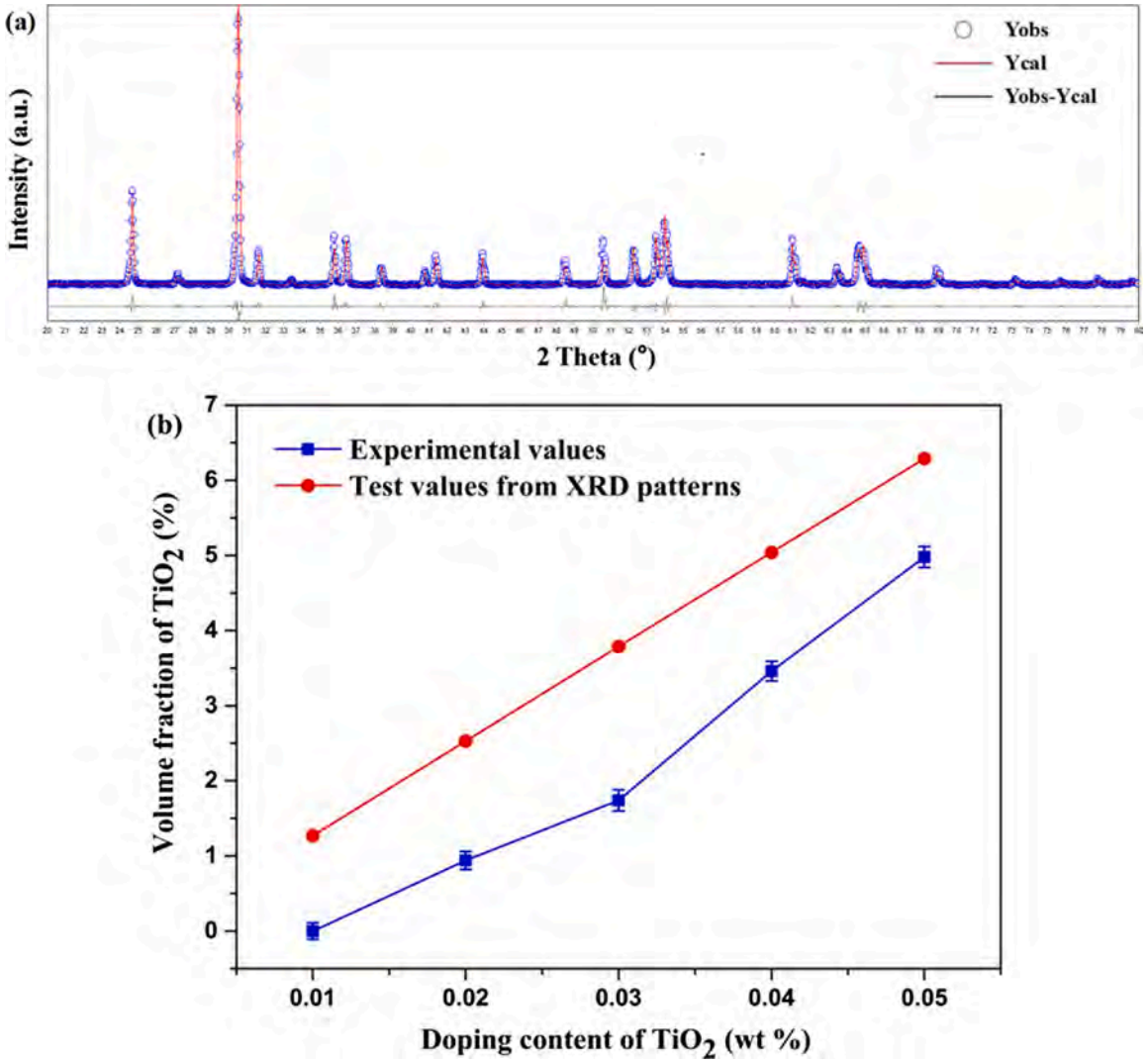

Fig. 3. (a) XRD refinement results for the ZTGN-0.04TO-ZTGN ceramic. (b) Volume fraction of TiO_2 in the ZTGN-xTO-ZTGN ($0.01 \leq x \leq 0.05$) ceramics.

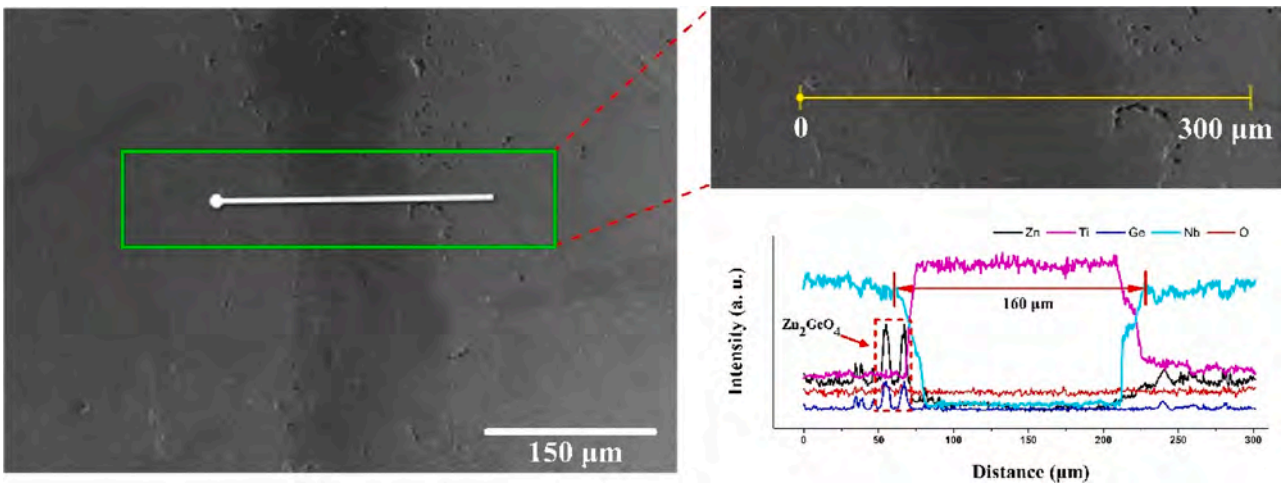

Fig. 4. SEM patterns of the random type and multi-layered type samples.

structure. However, due to the limited accuracy of the XRD test, the components of the transition phase with a lower content are almost undetectable. With a continuous increase in TiO_2 content, the errors between the theoretical values and the measured values gradually narrowed to a certain range, indicating that a relatively stable TiO_2 layer was formed when a sufficiently high TiO_2 content was reached. The relative densities of the $ZnTiNb_2O_8$ phase, Zn_2GeO_4 phase, and TiO_2 phase at x = 0.04 are approximately 96.8 %, 96.5 %, and 95.7 %, respectively. It can be reasonably speculated that the tri-layer co-fired ZTGN-0.04TO-ZTGN sample has a high relative density when sintering at 1120 ℃ for 6 h.

Fig. 4 shows the fractured surface micrographs of the ZTGN-0.04TO-ZTGN tri-layer sample and the EDS results of the selected line. As shown in Fig. 4, it can be observed that the boundary between the $ZnTi_{0.97}Ge_{0.03}Nb_2O_8$ layer and TiO_2 layer is unclear, the connection is relatively dense, and there are no traces of microcracks or large stomata. This result further indicates that the ZTGN-0.04TO-ZTGN tri-layer sample has great sintering quality. Meanwhile, a few spiculate grains formed by Zn_2GeO_4 penetrate the interfaces between the layers, which also improves the stability of the tri-layer structure to some extent. According to the EDS analysis results, a relatively complete TiO_2 layer (interlayer) and transition layer (interface) appear between the ZTGN layers, and the width is approximately 160 μm. At the interface, the diffusions of Zn, Nb, and Ti are restricted to a relatively narrow region between the different layers. Therefore, the tri-layer structure can effectively avoid chemical reactions between $ZnTi_{0.97}Ge_{0.03}Nb_2O_8$ and TiO_2, improving the microwave dielectric properties.

The microwave dielectric properties of tri-layer ZTGN-xTO-ZTGN samples with different TiO_2 contents are measured and compared with the theoretical values, as shown in Fig. 5. Based on the parallel model, the theoretical values of the microwave dielectric properties of the samples can be calculated by the following equations [13–14, 24–25]:

$$\varepsilon_r = V_1\varepsilon_1 + V_2\varepsilon_2 \tag{2}$$

$$\tan\delta = \frac{V_1\varepsilon_1\tan\delta_1 + V_2\varepsilon_2\tan\delta_2}{\varepsilon} \tag{3}$$

$$\tau_f = \frac{V_1\varepsilon_1\tau_f 1 + V_2\varepsilon_2\tau_f 2}{\varepsilon} \tag{4}$$

where V_1 and V_2, ε_1 and ε_2, $\tan\delta_1$ and $\tan\delta_2$, τ_{f1} and τ_{f2} present the volume fractions, the dielectric constants, the dielectric losses, and the τ_f values of the total system, phase 1, and phase 2, respectively. The Q values are nearly equal to the inverse of $\tan\delta$, and then the $Q\times f$ values of the composite samples can be predicted. The data required for the calculation of the microwave dielectric properties are shown in Table 1 and Fig. 3b. The overall trends of the measured and theoretical curves are similar (Fig. 5), although the experimental values are higher than the predicted results for the dielectric constant. The deviation between the theoretical values and the measured values increases with increasing TiO_2 content (Fig. 5a). When the mass of TiO_2 is less than 0.03 g, the theoretical value of the dielectric constant of the system is slightly less than the measured value. As the TiO_2 content continuously increases (>0.3 g), a relatively stable TiO_2 layer can be formed, and the deviation between the theoretical values and the measured values decreases.

The ceramic sample prepared in this paper is equivalent to a cylindrical dielectric resonator operating in $TE_{01}\delta$ mode. In this working mode, the inner wall of the medium is approximated as a magnetic wall. At this time, the direction of the magnetic field is perpendicular to the direction of the electric field. Based on the law of refraction, the dielectric constant of the ceramic sample (ε_r) and the incidence (θ_i) and refraction (θ_t) angles of the electromagnetic wave are related as follows [8,26]:

$$\sqrt{\varepsilon_r}\sin\theta_i = \sin\theta_t \tag{5}$$

Under the ideal resonance condition, θ_t is 90°, and the incident wave in the medium is reflected back to the medium, forming a standing wave. Therefore, most of the electric field is concentrated in the medium block, and θ_i satisfies the following relation [8,27]:

$$\theta_i = \theta_c = \sin^{-1}\left(\frac{1}{\sqrt{\varepsilon_r}}\right) \tag{6}$$

where θ_c is the critical angle of the incident electromagnetic wave, which presents the minimum incident angle when only reflection occurs. According to the relation above, the critical angle decreases with increasing dielectric constant. This means that the greater the dielectric constant of the materials, the easier all-reflection occurs, and the closer the inner wall of the medium is to the magnetic wall; thus, the electric field is more easily bounded in the high-permittivity dielectric materials. This means that the electric field lines are more densely distributed in the dielectric layer with a high dielectric constant.

Thus, the errors (as shown in Fig. 5a) result from two factors. First, the macroscopic dielectric constant of ZTGN is somewhat different from that of the rutile phase TiO_2 and the transition layer. Second, the microstructure formed by Zn_2GeO_4 possesses a low dielectric constant ($\varepsilon_r \sim 7$). This enhances the electric field distribution in the rutile phase TiO_2 and the interface between the different layers, avoiding the deterioration of the dielectric constant of the system under the normal tri-layer composite conditions. Fig. 5b and c show the $Q\times f$ values and τ_f values as a function of TiO_2 content, respectively. Due to the diversity of the dielectric constant between different layers, the reflection loss

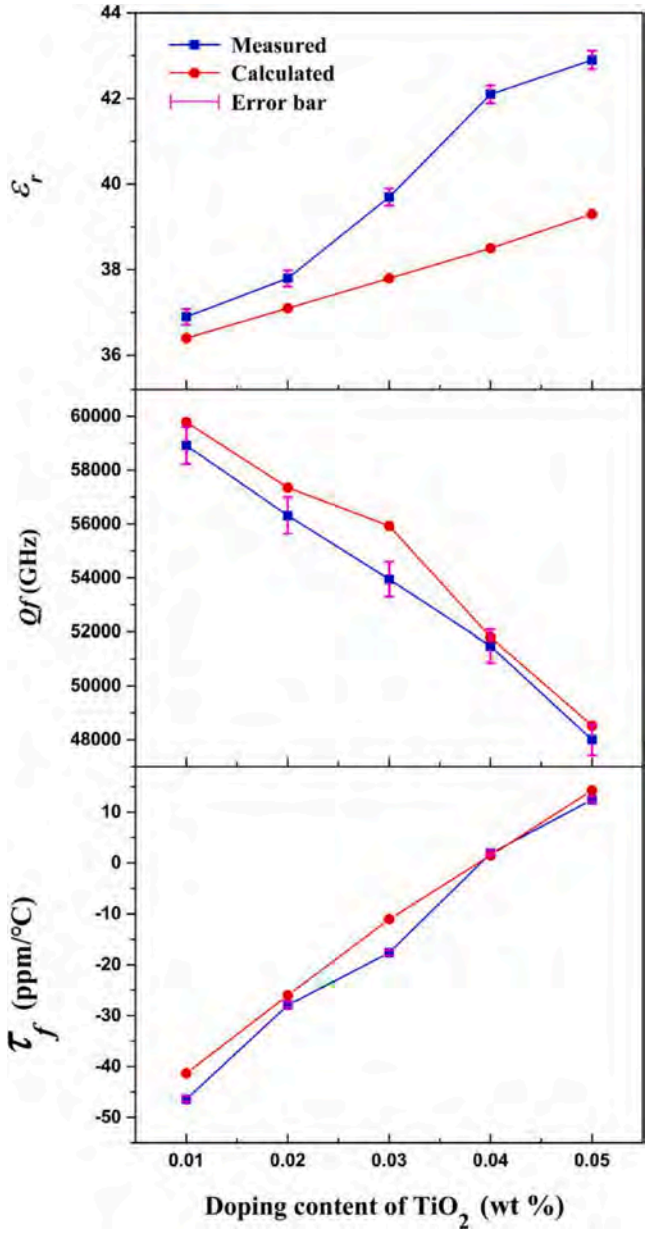

Fig. 5. Microwave dielectric properties of the tri-layer ZTGN-TO-ZTGN samples as a function of mass fractions of TiO_2.

cannot be ignored, which makes the Q×f values of the system slightly lower than the theoretical values. In addition, the measured values of the temperature coefficient of resonance frequency (τ_f) fit well with the theoretical values, and a near zero τ_f can be obtained when the mass ratio of TiO_2 is 0.04.

A summary of the Q×f value versus τ_f plot for $ATiNb_2O_8$-based and $AZrNb_2O_8$-based MWDCs is shown in Fig. 6, and some detailed values are listed in Table 2. Except for this work, other $ATiNb_2O_8$-based and $AZrNb_2O_8$-based MWDCs are prepared by random mixed synthesis. In comparison to the microwave dielectric performances described in previous studies, we can find that the performance of the tri-layer ZTGN-TO-ZTGN composite ceramics is superior. This study reports an excellent Q×f value and a large dielectric constant, which is compared with the study of systems with near-zero τ_f (Fig. 6 and Table 2).

Thus, in the present work, we have put forward a strategy to improve the microwave dielectric performance of conventional materials systems and provide a direction for the preparation of high-performance microwave dielectric ceramic materials based on available materials,

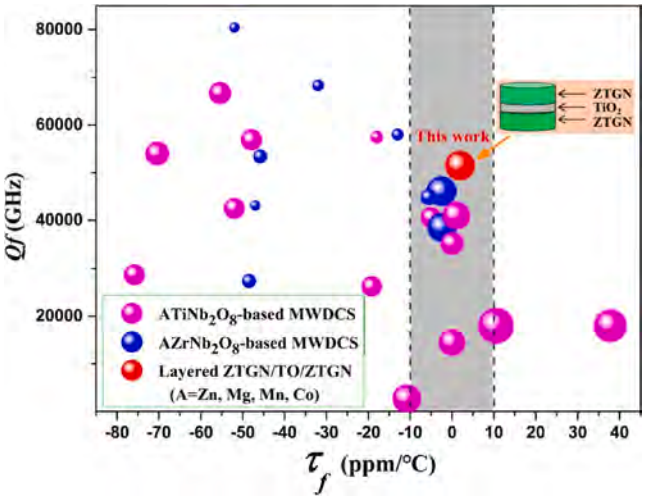

Fig. 6. Summary of the Q×f value versus τ_f plot for $ATiNb_2O_8$-based and $AZrNb_2O_8$-based MWDCs (the larger the ball in the figure, the greater the dielectric constant of the dielectric ceramic) [3,4,12,28–42].

Table 2
The microwave dielectric properties of samples prepared by the layered process and conventional mixed process.

Materials	S.T. (°C)	ε_r	Q×f (GHz)	τ_f (ppm/°C)	Ref.
$ZnTiNb_2O_8$	1120	34.3	42,500	−52	[12]
$MgTiNb_2O_8$	1000	33.8	26,260	−19.2	[30]
$0.63MgZrNb_2O_8$-$0.37TiO_2$	1300	43	46,110	−2.5	[31]
$Zn_{0.9}Mn_{0.1}ZrNb_2O_8$	1200	29.43	44,900	−5.61	[32]
$0.3ZnZrNb_2O_8$-$0.7TiO_2$	1150	41.4	38,500	−2.4	[35]
$MgZrNb_2O_8$	1250	26.54	57,477	−17.96	[37]
$Zn_{0.9}Mg_{0.1}ZrNb_2O_8$	1200	27.82	53,400	−45.82	[39]
$Zn_{0.7}Co_{0.3}TiNb_2O_8$	1075	35.93	35,125	0	[41]
ZTGN-0.04TO-ZTGN	1120	42.1	51,477	+1.9	This work

further adapting to the strict requirements for 5 G wireless communication devices.

4. Conclusion

Tri-layer ZTGN-TO-ZTGN composite ceramics were prepared and compared with random distribution-type ZTGN-TO composite ceramics. It is worth mentioning that the measured ε_r is higher than the theoretical values calculated by the parallel model. In contrast to the random distribution type ZTGN-TO, this architecture can achieve a nearly 50 % increase in the Q×f value, and the dielectric constant does not deteriorate significantly. The excellent performance is attributed to the stable tri-layer structure design. In this tri-layer structure, the existence of the stable TiO_2 layer (interlayer) and the microstructure formed by Zn_2GeO_4 enhance the distribution of the electric field in the region with a high dielectric constant and avoid the deterioration of the dielectric constant. In addition, the tri-layer structure design can largely avoid the occurrence of unexpected chemical reactions between the composite components. In conclusion, a near-zero τ_f (+1.9 ppm/°C) with high ε_r (42.1) and high Q×f (51,477 GHz) can be achieved in the tri-layer ZTGN-TO-ZTGN ceramic when the mass fraction of the TiO_2 layer is 0.04 wt% after sintering at 1120 °C for 6 h.

Declaration of Competing Interest

We ensure that the named authors have no conflict of interest with respect to finance and otherwise in this paper.

Acknowledgements

This work is supported by the National Natural Science Foundation of China (Grant Nos. 61701338, 61671326), and Natural Science Foundation of Tianjin City (Grant No. 18JCQNJC01300). The SEM work was done at the Institute for New Energy and Low-Carbon Technologies, Tianjin University of Technology, Tianjin, China.

References

[1] B. Ullah, W. Lei, Y.F. Yao, X.C. Wang, X.C. Wang, U.R. Muneeb, W.Z. Lu, Structure and synergy performance of (1-x)$Sr_{0.25}Ce_{0.5}TiO_3$-xLa($Mg_{0.5}Ti_{0.5}$)O_3 based microwave dielectric ceramics for 5G architecture, J. Alloys. Compd. 763 (2018) 990–996.

[2] G. Wang, D.N. Zhang, F. Xu, X. Huang, Y. Yang, G.W. Gan, Y.M. Lai, Y.H. Rao, C. Liu, J. Li, L.C. Jin, H.W. Zhang, Correlation between crystal structure and modified microwave dielectric characteristics of Cu^{2+} substituted $Li_3Mg_2NbO_6$ ceramics, Ceram. Int. 45 (8) (2019) 10170–10175.

[3] Q.J. Mei, C.Y. Li, J.D. Guo, H.T. Wu, Synthesis, characterization, and microwave dielectric properties of ixiolite-structure $ZnTiNb_2O_8$ ceramics through the aqueous sol-gel process, J. Alloys. Compd. 626 (2015) 217–222.

[4] H.B. Bafrooei, E.T. Nassaj, T. Ebadzadeh, Sintering behavior and microwave dielectric properties of nano zinc niobate powder, Ceram. Int. 40 (2014) 14463–14470.

[5] G. Wang, J. Jiang, Z.M. Dou, F. Zhang, T.J. Zhang, Sintering behavior and microwave dielectric properties of 0.67$CaTiO_3$-0.33$LaAlO_3$ ceramics modified by B_2O_3-Li_2O-Al_2O_3 and CeO_2, Ceram. Int. 42 (9) (2016) 11003–11009.

[6] M.H. Weng, C.T. Liauh, S.M. Lin, H.H. Wang, R.Y. Yang, Sintering behaviors, microstructure, and microwave dielectric properties of $CaTiO_3$-$LaAlO_3$ ceramics using CuO/B_2O_3 additions, Materials 12 (24) (2019) 4187.

[7] M.T. Sebastian, R. Ubic, H. Jantunen, Low-loss dielectric ceramic materials and their properties, Int Mater Rev. 60 (2015) 392–412.

[8] M.T. Sebastian, Dielectric Materials for Wireless Communication. Kidlington, Elsevier, UK, 2010.

[9] I.M. Reaney, D. Iddles, Microwave dielectric ceramics for resonators and filters in mobile phone networks, J. Am. Ceram. Soc. 89 (2006) 2063–2072.

[10] K. Wakino, Recent development of dielectric resonator materials and filters in Japan, Ferroelectrics. 91 (1989) 69–86.

[11] T. Tsunooka, M. Androu, Y. Higashida, H. Sugiura, H. Ohsato, Effects of TiO_2 on sinterability and dielectric properties of high-Q forsterite ceramics, J. Eur. Ceram. Soc. 23 (2003) 2573–2578.

[12] D.W. Kim, D.W. Kim, K.S. Hong, Phase relations and microwave dielectric properties of $ZnNb_2O_6$-TiO_2, J. Mater. Res. 15 (2000) 1331–1335.

[13] W.J. Luo, L.X. Li, B.W. Zhang, J.L. Qiao, The mechanism of microwave response in layer-cofired $Zn_3Nb_2O_8$-TiO_2-$Zn_3Nb_2O_8$ ceramic architecture, J. Alloys. Compd. 824 (2020), 153978.

[14] Y. Zhang, Y. Zhang, B.J. Fu, M. Hong, M.Q. Xiang, Z.A. Liu, J.X. Leng, Microstructure and microwave dielectric properties of $MgNb_2O_6$-$ZnTa_2O_6$ composite ceramics prepared by layered stacking method, J Mater Sci: Mater Electron. 25 (2014) 5475–5480.

[15] Y.C. Liou, Y.C. Wu, Microwave dielectric properties of $ZnNb_2O_6$-$SrTiO_3$ stacked resonators, J Electron Mater. 46 (4) (2017) 2387–2392.

[16] J. Zhang, Y. Luo, Z.X. Yue, L.T. Li, High-Q and temperature-stable microwave dielectrics in layer cofired $Zn_{1.01}Nb_2O_6/TiO_2/Zn_{1.01}Nb_2O_6$ ceramic architectures, J. Am. Ceram. Soc. 102 (2019) 342–350.

[17] J. Zhang, Y. Luo, Z.X. Yue, L.T. Li, $MgTiO_3/TiO_2/MgTiO_3$: An ultrahigh-Q and temperature-stable microwave dielectric ceramic through cofired trilayer architecture, Ceram. Int. 44 (2018) 21000–21003.

[18] A. Baumgarte, R. Blachnik, Isothermal sections in the systems ZnO-AO_2-Nb_2O_5 (A=Ti, Zr, Sn) at 1473 K, J. Alloys. Compd. (210) (1994) 75–81.

[19] D.W. Kim, D.W. Kim, K.S. Hong, Control of microwave dielectric properties in 0.42$ZnNb_2O_5$-0.58TiO_2 ceramics by the quantitative analysis of phase transition, J. Mater. Res. 33 (6) (2000) 1331–1335.

[20] W.J. Luo, L.X. Li, S.H. Yu, Z. Sun, B.W. Zhang, F. Xia, Structual, Raman spectroscopic and microwave dielectric studies on high-Q materials in Ge-doped $ZnTiNb_2O_8$ systems, J. Alloys. Compd. 741 (2018) 969–974.

[21] S.P. Wu, J. Ni, J.H. Luo, X.H. Ding, Preparation of $ZnNb_2O_6$-TiO_2 microwave dielectric ceramics for multi-layer cofired component, Mater. Chem. Phys. 117 (1) (2009) 307–312.

[22] E.S. Kim, D.H. Kang, Relationships between crystal structure and dielectric properties of $(Zn_{1/3}B^{5+}_{2/3})_xTi_{1-x}O_2$ (B^{5+}=Nb, Ta) ceramics, Ceram. Int. 34 (2008) 883–888.

[23] D.W. Kim, K.H. Ko, D.K. Kwon, K.S. Hong, Origin of microwave dielectric loss in $ZnNb_2O_6$-TiO_2, J. Am. Ceram. Soc. 85 (5) (2010) 1169–1172.

[24] J. Guo, D. Zhou, H. Wang, X. Yao, Microwave dielectric properties of (1−x) $ZnMoO_4$-xTiO_2 composite ceramics, J. Alloys. Compd. 509 (2011) 5863–5865.

[25] L.J. Cheng, S.W. Jiang, Q. Ma, Z.G. Shang, S.J. Liu, Sintering behavior and microwave properties of dense 0.7$CaTiO_3$-0.3$NdAlO_3$ ceramics with sub-micron sized grains by spark plasma sintering, Scripta Mater. 115 (2016) 80–83.

[26] R.D. Richtmeyer, Dielectric resonators, J. Appl. Phys. 15 (1939) 391–398.

[27] P.V. Bijumon, M.T. Sebastian, P. Mohanan, Experimental investigations and three dimensional transmission line matrix simulation of $Ca_{5-x}A_xB_2TiO_{12}$ (A=Mg, Zn, Ni and Co; B=Nb and Ta) ceramic resonators, J. Appl. Phys. 98 (12) (2005), 124105.

[28] Q.W. Liao, L.X. Li, Structural dependence of microwave dielectric properties of ixiolite structured $ZnTiNb_2O_8$ materials: crystal structure refinement and Raman spectra study, Dalton Trans. 41 (2012) 6963–6969.

[29] Y. Lei, Y.S. Yin, Y.C. Liu, Preparation and properties of $ZnTiNb_2O_8$microwave dielectric cramics, Adv Mater Res. 217-208 (2011) 1235–1238.

[30] Q.J. Mei, C.Y. Li, J.D. Guo, H.T. Wu, Synthesis, characterization, and microwave dielectric properties of ternary-phase ixiolite-structure $MgTiNb_2O_8$ ceramics, Mater. Lett. 145 (2015) 7–10.

[31] J. Zhang, R.Z. Zuo, Y. Cheng, Relationship of the structural phase transition and microwave dielectric properties in $MgZrNb_2O_8$-TiO_2 ceramics, Ceram. Int. 42 (2016) 7681–7689.

[32] J.X. Bi, C.H. Yang, H.T. Wu, Correlation of crystal structure and microwave dielectric characteristics of temperature stable $Zn_{1-x}Mn_xZrNb_2O_8$ ($0.02\leq x\leq 0.1$) ceramics, Ceram. Int. 43 (2017) 92–98.

[33] H.T. Wu, Z.B. Feng, Q.J. Mei, J.D. Guo, J.X. Bi, Correlations of crystal structure, bond energy and microwave dielectric properties of $AZrNb_2O_8$ (A= Zn, Co, Mg, Mn) ceramics, J. Alloys. Compd. 648 (2015) 368–373.

[34] Z.B. Feng, C.F. Xing, J.X. Bi, Sintering characteristics and microwave dielectric properties of low loss $CoZrNb_2O_8$ ceramics achieved by reaction sintering process, J. Alloys. Compd. 686 (2016) 923–929.

[35] X.S. Lyu, L.X. Li, S. Zhang, H. Sun, B.W. Zhang, J.T. Li, M.K. Du, Crystal structure and microwave dielectric properties of novel (1-x)$ZnZrNb_2O_8$-xTiO_2 ceramics, Mater. Lett. 171 (2016) 129–132.

[36] M. Guo, S.P. Gong, G. Dou, D.X. Zhou, A new temperature stable microwave dielectric ceramics: $ZnTiNb_2O_8$ sintered at low temperatures, J. Alloys. Compd. 509 (2011) 5988–5995.

[37] H.L. Pan, C.F. Xing, J.X. Bi, X.S. Jiang, Y.X. Mao, H.T. Wu, Sintering characteristics and microwave dielectric properties of low loss $MgZrNb_2O_8$ ceramics achieved by reaction sintering process, J. Alloys. Compd. 687 (2016) 274–279.

[38] M. Xiao, S.S. He, J. Lou, P. Zhang, Influence of Ge^{4+} substitution for Zr^{4+} on the microwave dielectric properties of $Mg(Zr_{1-x}Ge_x)Nb_2O_8$ ($0\leq x\leq 0.4$) ceramics, Ceram. Int. 44 (2018) 21585–21590.

[39] Y.J. Niu, M.T. Liu, M.F. Li, J.X. Bi, H.T. Wu, Influence of Mg^{2+} substitution on the crystal structure and microwave dielectric properties of $ZnZrNb_2O_8$ ceramics, J. Alloys. Compd. 705 (2017) 399–404.

[40] D.H. Kim, C. An, Y.S. Lee, Microwave dielectric properties of ZnO-RO_2-TiO_2-Nb_2O_5 (R = Sn, Zr, Ce) ceramic system, J. Mater. Sci. Lett. 22 (2003) 569–571.

[41] Z.L. Huan, Q.C. Sun, Crystal structure and microwave dielectric properties of $(Zn_{1-x}Co_x)TiNb_2O_8$ ceramics, J. Alloys. Compd. 551 (2013) 630–635.

[42] J.H. Park, Y.J. Choi, S. Nahm, J.H.G. Park, Crystal structure and microwave dielectric properties of $ZnTi(Nb_{1-x}Ta_x)_2O_8$ ceramics, J. Alloys. Compd. 509 (2011) 6908–6912.